

Received November 4, 2020, accepted November 20, 2020, date of publication December 3, 2020,
date of current version December 17, 2020.

Digital Object Identifier 10.1109/ACCESS.2020.3042388

Near-Limit Kinetic Energy Harvesting From Arbitrary Acceleration Waveforms: Feasibility Study by the Example of Human Motion

ANDRII SOKOLOV¹, (Graduate Student Member, IEEE), DIMITRI GALAYKO^{2,3}, (Member, IEEE),
MICHAEL PETER KENNEDY¹, (Fellow, IEEE), AND ELENA BLOKHINA¹, (Senior Member, IEEE)

¹School of Electrical and Electronic Engineering, University College Dublin, Dublin 4, D04 C1P1 Ireland

²LIP6, CNRS, UMR 7606, Sorbonne Université, 75005 Paris, France

³Center for Nanoscience and Nanotechnology, CNRS, Université Paris-Saclay, 91120 Gif-sur-Yvette, France

Corresponding author: Elena Blokhina (elena.blokhina@ucd.ie)

This work was supported in part by the Science Foundation Ireland under Grant 13/IA/1979 and Grant 13/RC/2077.

ABSTRACT Kinetic energy harvesters have become a common power source for autonomous sensors operating at micro- and meso-scales. The conventional approach to kinetic energy harvesting is to assume that the proof mass of the mechanical component in an energy harvester is actuated by external motion produced by the sensor's environment. This approach, dominant since the beginning of micro-scale energy harvesting, has now resulted in the design of advanced, nonlinear harvesters suitable for non-harmonic vibrations produced by many systems of interest. In this paper, we present a feasibility study of an alternative approach to kinetic energy harvesting, where the motion of the proof mass is actively synthesized.

INDEX TERMS Energy harvesting, microelectromechanical systems, transducers, algorithm design and analysis, statistical learning, time series analysis.

I. INTRODUCTION

In many aspects, electronic engineering is driven by the concept of the Internet of Things (IoT) and the vision of the interconnected world. One of the key issues that impedes the roll-out of the next wave of the IoT is the issue of energy supply [1]–[3]. The current generation of sensors utilise chemical sources of energy (batteries). However, in many cases, the size of batteries exceeds that of a typical sensor. Moreover, as the number of connected devices increases, one needs more and more batteries to supply them. There has been a steady progress in decreasing the size of sensors and optimising their energy consumption. However, in order to expand the IoT, one also requires to increase the effectiveness of power sources per given volume.

Energy harvesting, in particular, kinetic energy harvesting, seems a very attractive solution to this problem since energy has many forms and is abundant in our environment. Kinetic energy harvesters (KEH) transform the kinetic energy of a vibrating environment to electricity. There are a number of different mechanisms facilitating energy transfer from the

mechanical domain to the electrical one, including electromagnetic transduction [4]–[6] (when electric current is generated due to variable magnetic flux according to Faraday's law), electrostatic transduction [7], [8] (when the capacitance of a variable capacitor is changed by external vibrations) the piezoelectric effect [9], [10] (when voltage is generated due to the deformation of a piezoelectric layer), and their combinations [11], [12].

However, the resonators used in any type of harvesters have an inherent problem related to their natural vibrational spectrum. Assuming that a resonator is linear (or weakly non-linear), it only generates a significant amount of power when actuated over a narrow band of frequencies around its resonant ones, with negligible power generated outside its frequency response band. The common approach to mitigate this problem is to utilise mechanical or electrically-induced nonlinearities to widen the frequency response of a resonator. However, in this case one can experience the problem of bi-modality (also known as bi-stability) when small changes in the actuation force can lead to a spontaneous “jump” from a high-power to low-power branch.

Therefore, it is reasonable to want to create a high-performance KEH which will self-tune to irregular

The associate editor coordinating the review of this manuscript and approving it for publication was Shaopeng Wu¹.

aperiodic vibrations (for example human walking, running or any other typical activity). The main idea of this approach is to use an energy harvester with a strong coupling between the electrical and mechanical domains and to control the motion of the resonator in order to convert as much energy as possible. The concept of the energy harvester operating according to this principle is called the Near-Limit Kinetic Energy Harvester (NLKEH) [13], [14] since the power produced by it approaches the maximum for a given system.

The aim of this paper is to analyse environment vibration patterns for applications that are compatible with Near Limit Energy Harvesting and to investigate its feasibility. To do so, we introduce the concept of the maximum energy and power that may be converted from an arbitrary acceleration waveform using a given transduction mechanism. We investigate a range of vibration patterns generated from different human activities and analyse what energy can be extracted from them. As we will show, the implementation of Limit Energy Harvesting requires predictive control. For this reason, we are interested to understand the characteristics of these patterns, including their correlation properties.

This paper is organised as follows. Section II describes a mathematical formalism underlying the NLKEH. Section III discusses a methodology to collect acceleration pattern data and techniques to analyse the data including its Lyapunov exponents, correlation dimension and entropy. Section III-B is dedicated to the investigation of self-similarity of the signals. This is an important aspect of the NLKEH since the required predictive control can be effectively implemented for signals that display a clear pattern. Finally, in Section IV an algorithm of statistical learning is used to estimate the amount of energy that is convertible by the NLKEH. Conclusions and discussions are given in Section V.

II. NEAR LIMIT KINETIC ENERGY HARVESTERS

The first generation of kinetic energy harvesters (KEHs), proposed over a decade ago (see review [15]), offered a fundamental idea of how to derive energy from the environment. Unfortunately, this seminal paradigm was developed for harmonic or periodic vibrations rather than for irregular vibrations of the type that are usually observed in real-life applications. Over the following decade, the development of kinetic energy harvesting technique was aimed at extending the frequency band of harvesters to incorporate more complex (and even quasi-random and impulse like) acceleration waveforms. Since the study [16], the latest generation of KEHs is wideband with resonators employing mechanical nonlinearities, frequency tuning and frequency up-conversion effects, able to respond to kinetic motion over a very large range of input frequencies. This has potentially opened up applications in irregular vibrating environments, including human motion. The construction of the KEH implies the existence of a mechanical domain with a vibrating resonator, an electrical domain with a control and power management system and an interplay between them using the transduction mechanism (Fig. 1(a)). Wideband KEHs employing

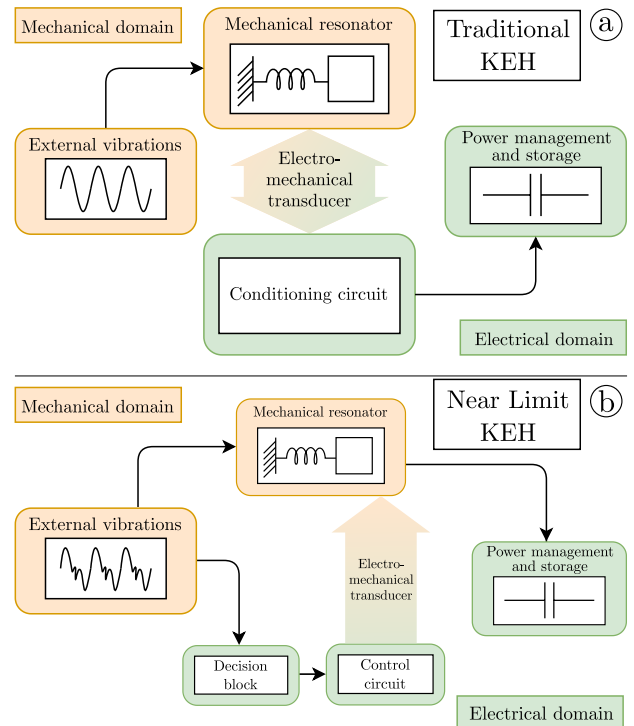


FIGURE 1. The high level block diagram of the kinetic energy harvester with an arbitrary transducer: (a) Conventional kinetic energy harvester and (b) Near-limit kinetic energy harvester.

nonlinear resonators have been implemented at a miniature scale using electromagnetic [4]–[6], piezoelectric [9], [10] and electrostatic [7], [8], [17] transduction mechanisms. While the number of publications in this domain has increased exponentially over recent years, research into the full integration of kinetic energy harvesters into real applications continues. The high level block diagram of a traditional energy harvester can be summarised as shown in Fig. 1(a). External vibrations cause the motion of a mechanical resonator (proof mass oscillating on an elastic spring). Since the aim is to convert energy into “electric” form, there are several types of available transducers that can transform the mechanical energy of the vibrations to the electric domain. A power management circuit is added to optimise the process and store energy.

The paradigm of near-limit kinetic energy harvesting utilises an active control of a trajectory generated by the proof mass and is based on a *non-resonant* principle. This method is developed to harvest energy from arbitrary vibration waveforms. Compared to the classic high-level diagram shown in Fig. 1(a), it requires an additional decision block that will generate an active force on the proof mass to ensure that its (proof mass) motion follows an optimal trajectory and results in maximal power converted (Fig. 1(b)). As we will discuss later in this section, the optimal control requires the knowledge of acceleration waveform properties. For this reason, the analysis of patterns and correlations in acceleration waveforms is the main focus of this feasibility study. In terms of the feasibility of the optimal control, we note that in fact

TABLE 1. Typical parameters of a microscopic kinetic energy harvester with acceleration magnitude and frequency taken as those of a typical human walking waveform.

Displacement limit (X_{lim})	25 mm
Proof mass (m)	1 g
External acceleration (A_{ext})	9.8 m/s ²
External frequency (f_{ext})	1 Hz

all transducers generate a force acting on the proof mass. In the case of a strong coupling between the electrical and mechanical domain, this force is significant and modifies the mechanical trajectory of the resonator. It may induce strong nonlinearity and even distort the frequency response of a harvester [17], [18]. However, the shape of the transducer's force generated by conventional (passive) electrical interfaces is, in most cases, far from the optimal one, such as that required to maximize the converted power.

Let us briefly outline the mathematical foundation of the NLKEH and compare it with the conventional formula developed for harmonic acceleration waveforms. The maximum power that can be converted from a harmonic vibration of a kinetic energy harvester can be expressed by the following formula [19]:

$$P_{lim} = 4mA_{ext}f_{ext}X_{lim}, \quad (1)$$

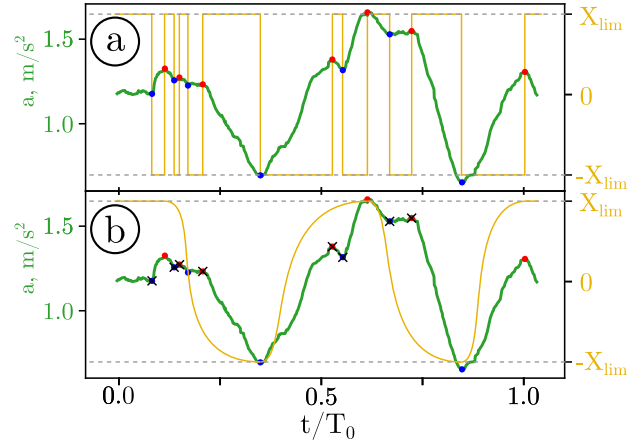
where m is the resonator's mass, A_{ext} is the external amplitude of the harmonic vibrations, f_{ext} is the frequency of the external vibrations and X_{lim} is the distance which limits the motion of the proof mass. Such a maximum power is converted if the mobile mass toggles between two possible extreme positions allowed by the system geometry (X_{lim} and $-X_{lim}$) at each local maximum of the external acceleration. In the case of sinusoidal external vibrations, the mass toggles twice per period. Setting for an electromechanical silicon device a reference volume of 1 cm³, the corresponding device parameters are presented in Tab. 1: the calculated limit power is approximately 1 mW, and this is the fundamental limit for an absolutely ideal system driven by a harmonic oscillations.

In many practical applications, external vibrations can be of quite an irregular form. Reference [13] explains in detail how to obtain an expression for the maximum energy and power that can be extracted from an arbitrary irregular waveform. We will not present the derivation here, but simply state the result:

$$W_{lim} = 2X_{lim}m \sum_i (a_{ext,i}^{max} - a_{ext,i}^{min}). \quad (2)$$

Here $a_{ext,i}^{max}$ and $a_{ext,i}^{min}$ are consecutive pairs of a local maximum/minimum of external acceleration, where the maximum occurs just after a local minimum. Taking into account a time segment between the corresponding accelerations ($t_i^{max} - t_i^{min}$), it is easy to obtain the expression for the average power limit [13]:

$$P_{lim} = 2X_{lim}m \cdot \frac{\sum_i (a_{ext,i}^{max} - a_{ext,i}^{min})}{\sum_i (t_i^{max} - t_i^{min})}. \quad (3)$$


FIGURE 2. An example of an external acceleration pattern and the optimal trajectory of the proof mass a) in the case of the ideal system (if the proof mass can move much faster than external acceleration can change) b) in case of the realistic system, when the proof mass has delay, and therefore the control system has to skip some local extrema.

Note that, in the case of a harmonic external acceleration waveform, for each period of oscillation there is only one maximum and one minimum $a_{ext,i}^{max} = -a_{ext,i}^{min} = A_{ext}$, and $(t_i^{max} - t_i^{min})^{-1} = f_{ext}$; thus, it is fully transformed to (1). Plugging in the parameters of a typical harvester from Table 1 into equation (3), one can estimate the maximum power. It is important to understand that this is the upper limit; it cannot be reached by a realistic device due to various losses.

According to the NLKEH principle, the ideal trajectory of the proof mass that results in the converted power P_{lim} given by formula (3) in response to an input acceleration waveform $a_{ext}(t)$ is shown in Fig. 2(a). Ideally, an NLKEH harvester from Fig. 1(b) should be able to detect every maximum (shown by the red dots) and minimums (shown by the blue dots) of $a_{ext}(t)$ and toggle the proof mass at the corresponding instances of time. The ideal trajectory consists of segments when the displacement x is constant and changes from $-X_{lim}$ to X_{lim} when the acceleration waveform has an extremum.

We note that realistically it would not be possible (and also not 'profitable' in the context of energy conversion) to toggle the proof mass at *every* extrema. Firstly, extremum detection and operation of the conditioning circuit has an energy cost. If the energy provided by the input waveform between the given a_{max} and a_{min} is less than the energy cost to operate the toggling, one should not activate it. Secondly, the proof mass has a response time defined by its mechanical parameters and the strength of electromechanical coupling ('electrical' damping [17], [20]). Therefore, it will not be able to react instantaneously, even if we force it to toggle at every extremum. A realistic trajectory of the proof mass is shown in Fig. 2(b).

Hence, we arrive at the idea of extrema selection for NLKEH: this is achieved by a decision block (Fig. 1(b)). The aim of this block is to make a decision (to toggle or not to toggle the proof mass) when an extremum of the waveform a_{ext} occurs. Since the energy gain is a difference between the

energy converted during two neighboring toggles, the decision device needs to predict the value of the future extremum in order to estimate the gain. Such a prediction is only possible if the decision block learns from the history of the input acceleration waveform. The decision block drives the conditioning circuit to keep the current position of the proof mass at $+X_{lim}$ or $-X_{lim}$ or to alter it.

The problem addressed by this paper concerns the feasibility of the decision making device required by the NLKEH concept. The paper aims to answer if prediction and control are feasible for a typical acceleration waveform generated from human motion. The next sections are focused on the analysis of human motion in the context of the energy that can be converted from them. We study the dynamical properties, patterns, predictive model and learning algorithm as applied to the motion waveforms collected under different external conditions.

III. ANALYSIS OF PATTERN IN EXTERNAL VIBRATIONS GENERATED BY HUMAN MOTION

In this Section, we present an overview of the characteristics of typical patterns generated by human motion. The first step of this investigation is data collection and processing. As a source of acceleration waveforms, we have chosen walking and running as possible applications of NLKEH. The data collection procedure involved several people using different devices (in-built accelerometers in iPhone, Google Pixel and M5Stack motion sensor, Fig. 3). The collected data was labelled depending on the conditions of each experiment (for instance: person, location of the sensor, activity type, sensor type). The obtained data was consistent in the sense that there was no significant dependence on the type of sensor [21]. The data collection and processing procedure is summarised in Fig. 4.

There is a significant body of literature published in regard to time series analysis, with a large number of methods available for analysis and prediction [22]–[27]. Some methods are conventional in signal processing (Fourier transform, auto-correlation function, auto-regressive integrated moving average model (ARIMA), dynamic time warping), while other methods originate from the theory of dynamical systems (phase portraits, Lyapunov exponents, embedding or correlation dimensions). We will employ a combination of known techniques but also suggest another analysis and visualisation method that would allow us to identify patterns and similarity in these time series easily.

A. ANALYSIS OF ACCELERATION WAVEFORMS

We start with conventional techniques of time series analysis that include auto-correlation functions, Fourier transforms, correlation dimensions and ARIMA predictive modelling to investigate the correlation properties of such motion.

One of the traditional techniques showing the feasibility of the forecasting for time series is the calculation of the auto-correlation function (ACF) that shows the correlation between a signal and the same signal shifted by a time lag,

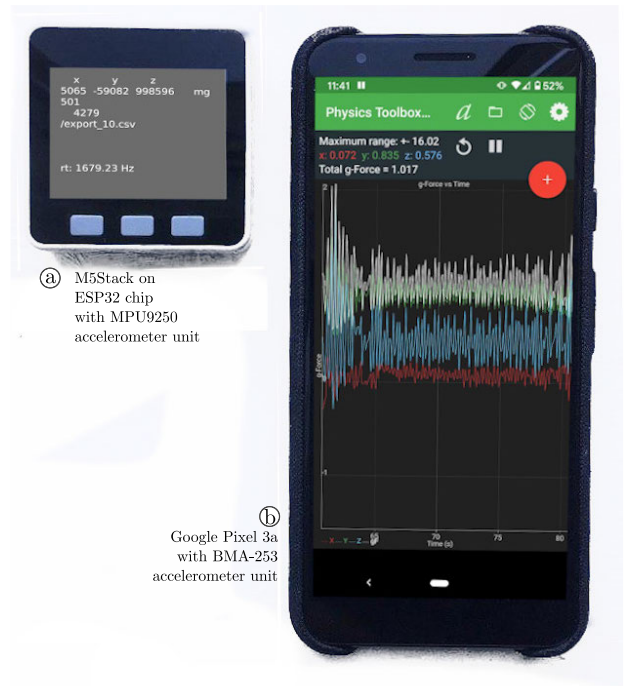


FIGURE 3. Measurement devices: (a) M5Stack on a ESP32 programmable (Arduino compatible) chip and a MPU9250 accelerometer-gyroscope sensor; (b) Google Pixel 3a Android smartphone with an BMA-253 sensor. The Physics Toolbox application was used to collect the data.

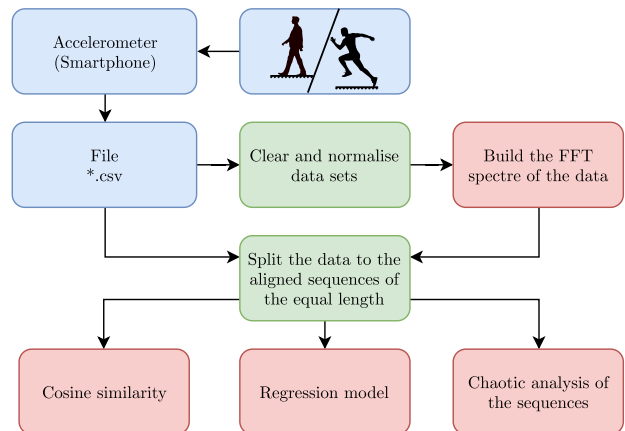


FIGURE 4. The summary of the algorithm used for data collection and processing including data filtering, obtaining its characteristic frequencies, regression models and similarity measure.

defined as:

$$\Psi(\tau) = \int_{t_{min}}^{t_{max}} f(t)f^*(t - \tau)dt, \quad (4)$$

where $f(t)$ is the waveform of a signal versus time, τ is the time lag, t_{min} and t_{max} are the time limits of the given time-series (ideally infinite). The analysis of the ACF calculated for the patterns of walking (when an accelerometer device is in a hand) reveals a slowly decaying function involving multiple frequencies with a dominant peak corresponding to one cycle of walking (two steps) and minor peaks corresponding to individual steps, Fig. 5(a), implying a significant degree of self-similarity in such a waveform. Patterns of

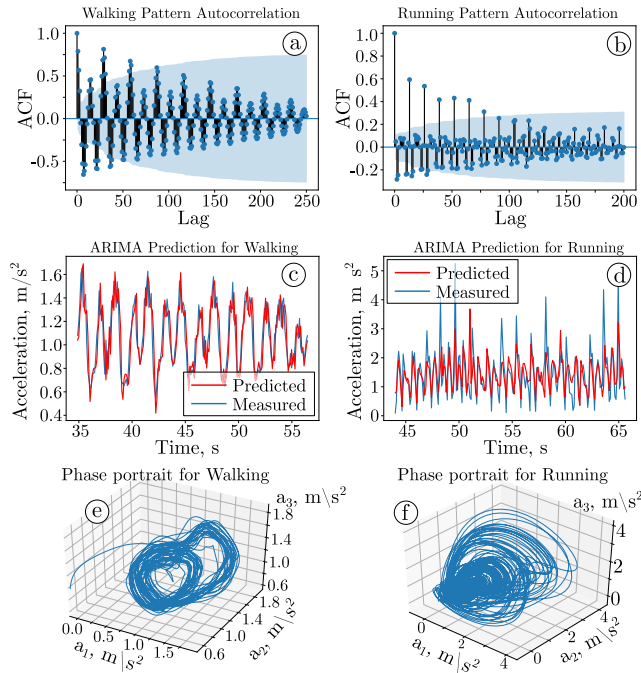


FIGURE 5. Comparison of running and walking acceleration patterns respectively: (a) and (b) Auto-correlation functions with a given time lag, dots and lines shows the ACF, blue region shows the reliability region; (c) and (d) Predictive modelling obtained from ARIMA models trained on the first 2/3 segment of the given data series and its comparison with the last 1/3 segment of the measured time series; (e) and (f) visualisation of the time series using phase portraits in the reconstructed state space.

running, as expected, show lower degree of self-correlation than walking ones (Fig. 5(b)). However, the correlation time between the ACF peaks are still clearly visible, implying that predictive models of walking and running time series are feasible.

A well-known demonstration of the feasibility of predictive modelling of a time series is the Autoregressive Integrated Moving Average (ARIMA) model [24]. This model $ARIMA(p, d, q)$ for the non-stationary time series X_t is built the following way:

$$\Delta^d X_t = c + \sum_{i=1}^p a_i \Delta^d X_{t-i} + \sum_{j=1}^q b_j \varepsilon_{t-j} + \varepsilon_t, \quad (5)$$

where ε_t is a stationary time series, c, a_i, b_j are parameters of the model, Δ^d is the operator of the time series difference of the d -order. This ARIMA model was trained on the first 2/3 of the recorded human motion time series, and then predictions made by this model for the last 1/3 of the time series were compared with the measured data. As one can see, the autoregressive models works well for both running and walking time series (Fig 5(c),(d)). This fact convinces us that it is possible to use these learning algorithms with these activities. However, the energy harvesting application should require less resource intensive algorithms than the ARIMA method.

It is also necessary to assess the possible chaotic properties of the data: a strongly chaotic dataset causes significant

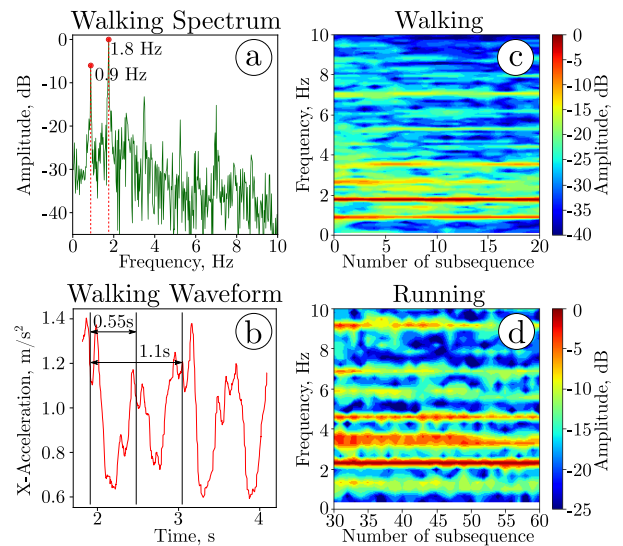


FIGURE 6. Fast Fourier Transformation (FFT) of the acceleration patterns: (a) FFT of the total walking data-set; (b) the corresponding walking oscillation that demonstrates two main frequencies; (c) FFT made with moving window along the time-scale, it is easy to see that all harmonics have similar amplitudes with time; (d) similar picture for the running acceleration pattern.

difficulties with predictions. For that, we need to calculate the embedding dimension of a pattern which, in many cases, is the same as correlation dimension of a data set [27]. The Grassberger-Procaccia algorithm [28] is available in many packages for data analysis. We use the *nolds* module in Python which correlation dimension ~ 1.8 for walking and ~ 2.3 for running.

The obtained correlation dimension allows us to draw the phase portrait (Fig. 5 (e),(f)) that shows a typical behaviour of chaotic attractor in case of running. In addition, we used the Rosenstein method [29] to calculate the highest Lyapunov exponent, which is the reciprocal to the characteristic time when a system becomes chaotic.

B. ANALYSIS OF PATTERNS TROUGH CROSS-SIMILARITY

As was highlighted before, the experimental data was obtained using a smartphone with an accelerometer. The experimental data was exported as coma separated values (*.csv) files, and then processed on a computer.

Despite the comfortable measurements, the usage of the smartphone has some drawbacks. The sequences were written with a resolution of 1 ms, however, because of the features of the internal clock of the phone, the extracted sequence contains gaps of 1 – 3 ms, nevertheless missing data could be restored by interpolation in order to build the discrete Fourier transform (DFT) spectrum of the system (Fig.6 (a)).

The analysis of the Fourier transformation can show the main frequency of the walking, and therefore to define the duration of the single step, as is shown in Fig. 6 (b). The building of the DFT spectra for different sub-sequences (Fig. 6 (c), (d)) also show that different parts of the signal has the same harmonics.

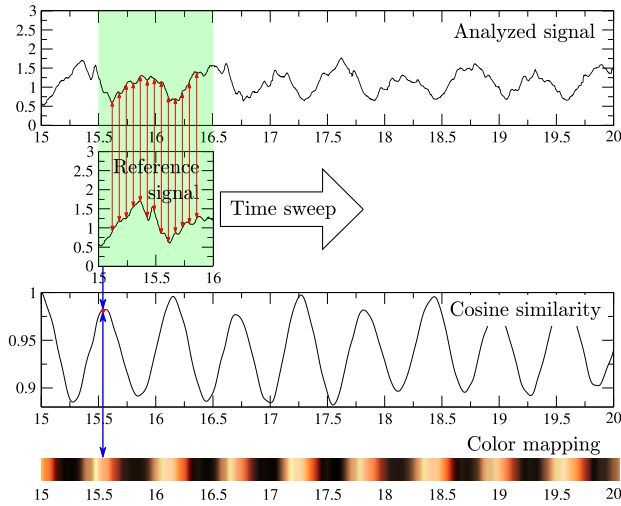


FIGURE 7. The figure shows schematic steps for building the cross-similarity map for the given sub-sequence. The top figure is the analysed signal, the next is the reference signal, it sweeps along the analysed signal, and for each configuration the cosine similarity is calculated and transformed to the colour-map.

Finally, to make sure that the given excitation has recognisable repeatable pattern we made the direct comparison between sub-sequences. A fast way to do this is to estimate the cosine similarity of the pairs of the sequences, which is a well-known tool in data science [30], [31]:

$$C = \frac{(\vec{x}_1, \vec{x}_2)}{|\vec{x}_1|^2 + |\vec{x}_2|^2}, \quad (6)$$

where \vec{x}_1 and \vec{x}_2 are vectors storing the two time series to be compared:

$$\vec{x}_i = (a_1^{(i)}, a_2^{(i)}, a_3^{(i)}, \dots, a_n^{(i)}). \quad (7)$$

Cosine similarity is a very useful quantity which allows us to understand if the measured signal has a repeatable pattern. To do this, one can use the following algorithm (Fig. 7):

- 1) Define the appropriate sub-sequence of the signal. The most convenient length of the sub-sequence corresponds to one period of the oscillation, which is found from the FFT analysis (Fig. 6)
- 2) Calculate the cosine similarity (6) between all different continuous sub-sequences of the initial sequence by using the time sweep.
- 3) Code the cosine similarity using a colour mapping (Fig. 7).
- 4) Repeat this for every sub-sequence, which corresponds to the vibration period, and build the full map of the cross-similarity (Fig. 8).

The analysis of the pattern’s cross-similarity shows that the given signal has a pronounced pattern in which one can identify a weak and a strong similarity (Fig. 8). This effect is caused by the fact that a walking person produces slightly different acceleration signals when taking steps with the left and the right legs.

The analysis of the given cross-similarity shows a similarity pattern in the data collected from a given activity

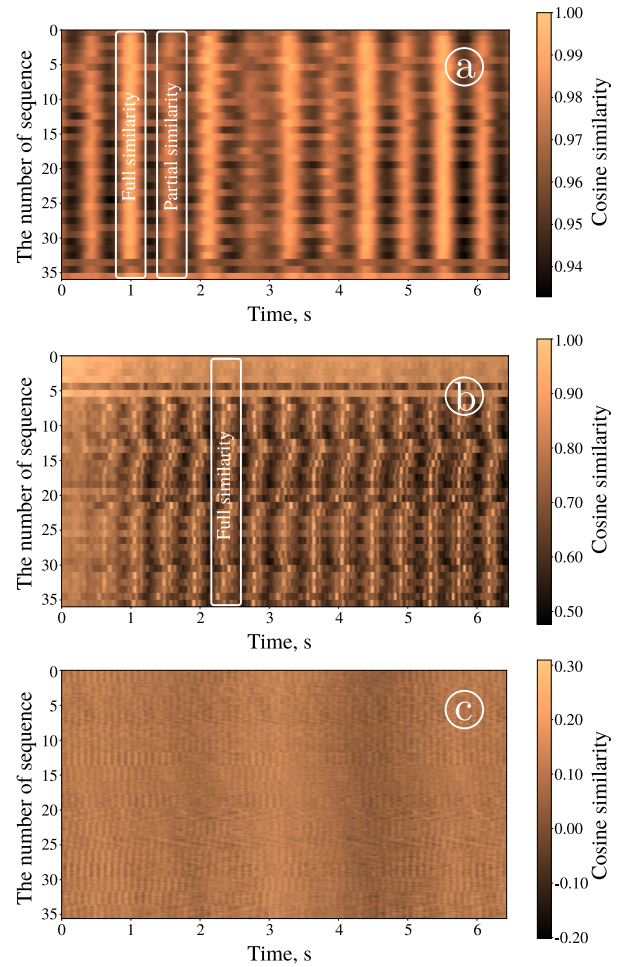


FIGURE 8. The cosine cross-similarity of the different motion activities. (a) The cross-similarity of walking. (b) The cross-similarity of running. (c) The mixed similarity where the running pattern is used as analysed, and the walking pattern was used as the reference.

and an absence of any correlations in the case of different motion patterns. That allows us to propose prediction algorithms that allow one to estimate the energy which can be converted by the near-limit energy harvester in the immediate future. This information will then be used to decide if it is worth ordering to toggle the mobile mass at a given detected extremum.

IV. DESCRIPTION OF THE PROPOSED DECISION ALGORITHM

In this section we propose a maximum/minimum selection algorithm to maximise the the energy extracted by a NLKEH, based on a prediction of the future of the sequence. The method is based on prior identification of aligned normalised sub-sequences of the external accelerations, which are used as a reference sequence. We propose the following algorithm for the extrema selection (Fig. 9):

- 1) Split the analysed signal into sub-sequences of equal length. The optimal length of such sub-sequence should be a multiple of the period of the signal, that can be

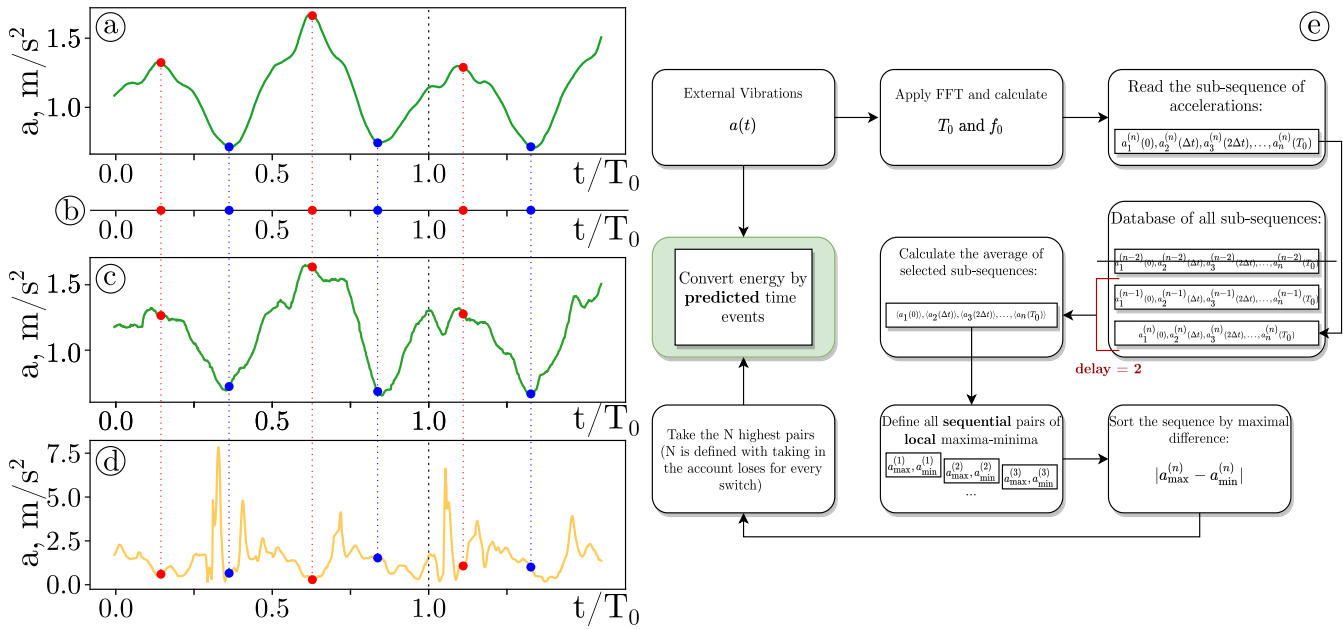


FIGURE 9. Demonstration of the learning method: a) the initial sample of the acceleration (walking pattern) b) the sequence of the maxima (red circles) and minima (blue circles) of the acceleration defined by the signal c) the sequence applied to the arbitrary walking signal d) the sequence applied to the arbitrary running signal. e) suggested learning algorithm starting from the measurements of the External Vibrations, and ending with an Energy Conversion.

defined by the FFT. The optional step is to apply a high-pass filter [32], [33] to the reference signal)

- 2) For each next sub-sequence we need to choose a number previous sub-sequences and calculate the reference waveform (Fig. 9 a) as an average over the given ensemble.
- 3) Identify all pairs of minima and maxima at the reference signal, and identify the relative time instances when they occur (Fig. 9 b).
- 4) In the reference signal, collect only the maxima and minima which maximise the net average converted power calculated as the difference between (3) and the power required to toggle. In the simplest case, this can be done by defining a threshold between the neighboring extrema. The sequence of minima/maxima defined at this step is called the “reference pattern”.
- 5) Superimpose the reference pattern (Fig. 9 (b)) with the other (non-reference) sub-sequences, and use the minima and maxima of the reference pattern to identify the time instants at which a toggle should be done on other sub-sequences (Fig. 9 (c),(d)). Due to the similarity between the sequences, the selected points will correspond to the maxima which should be selected for the toggling.

Step c) of the proposed algorithm consists of selecting the optimal extrema subset for NLKEH toggling in the reference sequence on the basis of the *whole (a posteriori) knowledge* of the sequence. This operation is not trivial, and we propose here a discussion about how it can be implemented. After that, we will show how the identified optimal sequence may be used to control the NLKEH.

A. A POSTERIORI SELECTION OF THE OPTIMAL EXTREMA SUBSET

After step 2) of the algorithm, we have the set $\epsilon = \{t_i, a_i\}$, $i \in [1, N]$, where t_i is the time and a_i is the value of the i^{th} extremum in the reference sub-sequence. Without loss of generality, we consider that for odd i all a_i are maxima and for even i all a_i are minima. Then the formula (2) gives the maximum energy W_N which can theoretically be converted from this vibration if the mass toggles at each extremum.

Now we suppose that, because of non-zero losses associated with toggling the mobile mass, we can only select $n < N$ “best” extrema, which will allow us to convert energy $W_n < W_0$. If the energy loss due to each toggling is δ , the net energy is given by:

$$W_{\text{net}; n} = W_n - n\delta. \quad (8)$$

Figure 10 (a) presents the convertible energy W_n as a function of n normalized by W_N (green curve) measured on vibrations issued from human walking. For small n the energy grows fast, since we select the “maximum-minimum” pair with the highest amplitude. For larger n we have to include maxima of minima of lower amplitude, and we end with insignificant extrema due to the noise, where the plot saturates. On the same plot we draw the loss function $n\delta$ (red curve).

The function W_n/W_N of Fig. 10 (a) is calculated for several sub-sequences, which allows one to see the statistical dispersion (uncertainty) of this measure.

Figure 10(b) represents the normalized net converted energy defined as $W_{\text{net} n}/W_N$. This plot shows the average net energy over *several* sub-sequences with error-bars

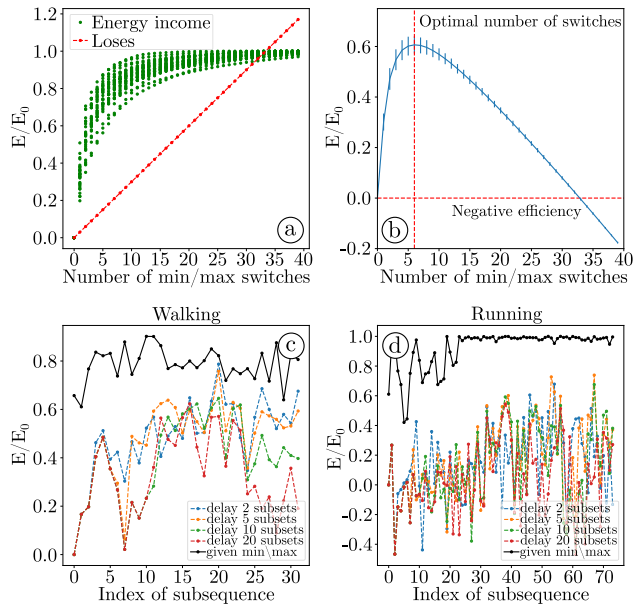


FIGURE 10. a) Normalized gross extracted energy versus the number of toggling over a sub-sequence. Losses are shown as the red line. b) Normalized net extracted energy versus the number of toggling over a sub-sequence. c, d) Normalized net energy obtained with walking, for different history depth of learning for vibrations issued from walking and running.

(99% confidence). This plot allows one to select the optimal number of toggling to maximize the net energy (6 toggling in this case). The identified optimum set of extrema is then used as the reference pattern in the step 4) of the algorithm presented above.

B. USE OF THE REFERENCE PATTERN FOR EXTREMA SELECTION IN FUTURE SEQUENCE

In this subsection we show how the reference pattern calculated from the reference previous sub-sequences is used to extract energy from future sub-sequences. We demonstrate the application of the algorithm to the vibration sequences resulting from two contexts: a walking human and a running human.

The results are summarized in Figures 10 c and d. On the vertical axis we present here the plot of the normalized net energy recovered from the vibrations. The horizontal axis is the index of the sub-sequence i inside the sequence, which can be interpreted as the discrete time iT_s , where T_s is the duration of the sub-sequence.

Our previous analysis shows that both walking and running acceleration vibrations change slightly with time; thus, the vibration history relevant for the prediction is limited in time. For this reason, for each sub-sequence i , the learning is performed with only k previous sub-sequences. For that, k previous subsequences are averaged in time, and the reference pattern is calculated on the averaged subsequence as explained in Sec. III-A. Figures 10 (c) and (d) show the results for $k = 2, 5, 10, 20$. For the sequences with index $i \leq k$, the learning has been performed on the first

TABLE 2. The estimations of the power which can be harvested by the KEH in normal linear regime and near-limit regime.

Value	Walking	Running
Power with harmonic approximation, mW	0.045	0.4
Maximal estimated power, mW	3.77	8.80
Power estimated with learning, mW	2.6	6.0

($i - 1$) sequences. Each plot shows the normalized energy extracted at each sub-sequence for each length of the learning history (the value of k).

The black plot presents the ideal maximum net energy which can be extracted from each sub-sequence. This value is calculated a posteriori, by application of the reference pattern which is calculated from the sub-sequence itself (not from the history). The difference between this ideal value and the energy extracted after a learning on the past provides a measure of the efficiency of the proposed method. Note that all learning curves start from 0-efficiency, this is because we do not have any information about the 1-st subset. It is easy to see that the efficiency of the proposed learning algorithm is much higher in the case of the walking pattern, with learning on 2-10 previous subsets. It has good agreement with the ACF of the signal (Fig. 5 (a),(c)).

However, the proposed algorithm has difficulties with the running pattern. One can see that proposed algorithm sometimes even produces a “negative” efficiency (see (2) if we assume the wrong points of accelerations as maxima and minima, such as $a_{ext,i}^{min} > a_{ext,i}^{max}$, for most instances of time, the oscillator will convert energy, vice versa, from the electrical domain to the mechanical one). It can be explained by the fact that in the case of running there is only a single huge peak that produces the maximal amount of energy, and it is really difficult to predict the position of the peak (it is weakly changing). It means that for running we need to develop a different learning algorithm that takes this features into account.

As one can see, the power estimated in the near-limit regime is much higher than in the linear regime. However, we should keep in mind that this estimate shows the upper limit of the harvested power, because some power should be used to tune the pattern of minima and maxima, and to switch to different regimes.

V. CONCLUSION

In this paper we analysed acceleration patterns of typical human activities (running and walking). We showed that the patterns are repeatable and weakly chaotic and therefore we can design a self-tuning system which will harvest the energy at certain time intervals. Finally, we introduced the concept of the learning efficiency and showed that it is growing with the time of learning. The numerical estimation showed that the proposed approach allows one to extract significantly greater power than the traditional linear KEH.

The next step of our investigation will be to focus on the implementation of this idea in a fabricated device based on the defined energy transition mechanism. There are several challenges related to this step — the influence of the

electro-mechanical coupling on the motion pattern of the resonator, estimation of the energy which is spent on the self-tuning and on toggling the mass and the energy required for on-chip machine learning.

Nevertheless, the proposed concept potentially offers a new path to high-efficiency kinetic energy harvesting.

REFERENCES

- [1] A. Raj and D. Steingart, "Power sources for the Internet of Things," *J. Electrochem. Soc.*, vol. 165, no. 8, pp. B3130–B3136, 2018.
- [2] I. Demirkol, D. Camps-Mur, J. Paradells, M. Combalia, W. Popoola, and H. Haas, "Powering the Internet of Things through light communication," *IEEE Commun. Mag.*, vol. 57, no. 6, pp. 107–113, Jun. 2019.
- [3] M. H. Miraz, M. Ali, P. S. Excell, and R. Picking, "A review on Internet of Things (IoT), Internet of everything (IoE) and Internet of nano things (IoNT)," in *Proc. Internet Technol. Appl. (ITA)*, Sep. 2015, pp. 219–224.
- [4] A. Sokolov, D. Mallick, S. Roy, M. P. Kennedy, and E. Blokhina, "Modelling and verification of nonlinear electromechanical coupling in micro-scale kinetic electromagnetic energy harvesters," *IEEE Trans. Circuits Syst. I, Reg. Papers*, vol. 67, no. 2, pp. 565–577, Feb. 2020.
- [5] D. Mallick, A. Amann, and S. Roy, "High figure of merit nonlinear micro-electromagnetic energy harvesters for wideband applications," *J. Microelectromech. Syst.*, vol. 26, no. 1, pp. 273–282, Feb. 2017.
- [6] B. Yang, C. Lee, W. Xiang, J. Xie, J. Han He, R. K. Kotlanka, S. P. Low, and H. Feng, "Electromagnetic energy harvesting from vibrations of multiple frequencies," *J. Micromech. Microeng.*, vol. 19, no. 3, Mar. 2009, Art. no. 035001.
- [7] H. Honma, Y. Tohyama, H. Mitsuya, G. Hashiguchi, H. Fujita, and H. Toshiyoshi, "A power-density-enhanced MEMS electrostatic energy harvester with symmetrized high-aspect ratio comb electrodes," *J. Micromech. Microeng.*, vol. 29, no. 8, Aug. 2019, Art. no. 084002.
- [8] B. John. (Feb. 2019). *A MEMS Device Harvests Vibrations to Power the IoT*. *IEEE Spectrum*. [Online]. Available: <https://spectrum.ieee.org/nanoclast/energy/renewables/a-mems-vibration-energy-harvester-for-the-iot>
- [9] O. Z. Olszewski, R. Houlihan, A. Blake, A. Mathewson, and N. Jackson, "Evaluation of vibrational PiezoMEMS harvester that scavenges energy from a magnetic field surrounding an AC current-carrying wire," *J. Microelectromech. Syst.*, vol. 26, no. 6, pp. 1298–1305, Dec. 2017.
- [10] S.-G. Kim, S. Priya, and I. Kanno, "Piezoelectric MEMS for energy harvesting," *MRS Bull.*, vol. 37, no. 11, pp. 1039–1050, 2012.
- [11] R. Houlihan, N. Jackson, A. Mathewson, and O. Z. Olszewski, "A study on the spatial dependence of a MEMS electromagnetic transducer," *J. Microelectromech. Syst.*, vol. 28, no. 2, pp. 290–297, Apr. 2019.
- [12] R. Hamid and M. R. Yuce, "A wearable energy harvester unit using piezoelectric–electromagnetic hybrid technique," *Sens. Actuators A, Phys.*, vol. 257, pp. 198–207, Apr. 2017.
- [13] D. Galayko, A. Karami, P. Basset, and E. Blokhina, "Kinetic energy harvesting for the IoT: Perspectives and challenges for the next decade," in *Proc. 25th IEEE Int. Conf. Electron., Circuits Syst. (ICECS)*, Dec. 2018, pp. 593–596.
- [14] E. Blokhina, A. Sokolov, X. Tian, and D. Galayko, "Pattern recognition in human motion for kinetic energy harvesting," in *Proc. 26th IEEE Int. Conf. Electron., Circuits Syst. (ICECS)*, Nov. 2019, pp. 81–84.
- [15] P. D. Mitcheson, E. M. Yeatman, G. K. Rao, A. S. Holmes, and T. C. Green, "Energy harvesting from human and machine motion for wireless electronic devices," *Proc. IEEE*, vol. 96, no. 9, pp. 1457–1486, Sep. 2008.
- [16] F. Cottone, H. Vocca, and L. Gammaitoni, "Nonlinear energy harvesting," *Phys. Rev. Lett.*, vol. 102, no. 8, 2009, Art. no. 080601.
- [17] P. Basset, E. Blokhina, and D. Galayko, *Electrostatic Kinetic Energy Harvesting*. Hoboken, NJ, USA: Wiley, 2016.
- [18] E. Blokhina, A. El Aroudi, E. Alarcon, and D. Galayko, *Nonlinearity in Energy Harvesting Systems: Micro- and Nanoscale Applications*. Springer, 2016.
- [19] P. D. Mitcheson, P. Miao, B. H. Stark, E. M. Yeatman, A. S. Holmes, and T. C. Green, "MEMS electrostatic micropower generator for low frequency operation," *Sens. Actuators A, Phys.*, vol. 115, nos. 2–3, pp. 523–529, Sep. 2004.
- [20] E. O'Riordan, A. Dudka, D. Galayko, P. Basset, O. Feely, and E. Blokhina, "Capacitive energy conversion with circuits implementing a rectangular charge-voltage cycle part 2: Electromechanical and nonlinear analysis," *IEEE Trans. Circuits Syst. I, Reg. Papers*, vol. 62, no. 11, pp. 2664–2673, Nov. 2015.
- [21] A. Jalal, M. A. K. Quaid, and M. A. Siddiqui, "A triaxial acceleration-based human motion detection for ambient smart home system," in *Proc. 16th Int. Bhurban Conf. Appl. Sci. Technol. (IBCAST)*, Jan. 2019, pp. 353–358.
- [22] B. Schelter, M. Winterhalder, and J. Timmer, *Handbook of Time Series Analysis*. Hoboken, NJ, USA: Wiley, 2006.
- [23] G. E. Box, G. M. Jenkins, G. C. Reinsel, and G. M. Ljung, *Time Series Analysis: Forecasting and Control*. Hoboken, NJ, USA: Wiley, 2015.
- [24] D. McDowall, R. McCleary, and B. J. Bartos, *Interrupted Time Series Analysis*. London, U.K.: Oxford Univ. Press, 2019.
- [25] A. H. Nayfeh and B. Balachandran, *Applied Nonlinear Dynamics: Analytical, Computational, and Experimental Methods*. Hoboken, NJ, USA: Wiley, 2008.
- [26] S. P. Kuznetsov, "Dynamical chaos and uniformly hyperbolic attractors: From mathematics to physics," *Physica-Uspekhi*, vol. 54, no. 2, p. 119, 2011.
- [27] V. S. Anishchenko, V. Astakhov, A. Neiman, T. Vadivasova, and L. Schimansky-Geier, *Nonlinear Dynamics of Chaotic and Stochastic Systems: Tutorial and Modern Developments*. Springer, 2007.
- [28] P. Grassberger and I. Procaccia, "Characterization of strange attractors," *Phys. Rev. Lett.*, vol. 50, no. 5, p. 346, Jan. 1983.
- [29] M. T. Rosenstein, J. J. Collins, and C. J. De Luca, "A practical method for calculating largest Lyapunov exponents from small data sets," *Phys. D, Nonlinear Phenomena*, vol. 65, nos. 1–2, pp. 117–134, May 1993.
- [30] W. Van Der Aalst, "Data science in action," in *Process Mining*. Berlin, Germany: Springer, 2016, pp. 3–23.
- [31] D. Cielien, A. Meysman, and M. Ali, *Introducing Data Science: Big Data, Machine Learning, and More, Using Python Tools*. Shelter Island, NY, USA: Manning Publications, 2016.
- [32] E. Schöll and H. G. Schuster, *Handbook of Chaos Control*, vol. 2. Hoboken, NJ, USA: Wiley, 2008.
- [33] D. Wu, N. Fang, C. Sun, X. Zhang, W. J. Padilla, D. N. Basov, D. R. Smith, and S. Schultz, "Terahertz plasmonic high pass filter," *Appl. Phys. Lett.*, vol. 83, no. 1, pp. 201–203, Jul. 2003.



ANDRII SOKOLOV (Graduate Student Member, IEEE) received the B.Sc. degree in computational physics and the M.Sc. degree in theoretical physics from Odessa National I.I. Mechnikov University, Ukraine, in 2009 and 2010, respectively. He is currently pursuing the Ph.D. degree with the School of Electrical and Electronic Engineering, University College Dublin, Ireland. He is the coauthor of publications on simulation of electromagnetic and electrostatic microelectromechanical systems and quantum systems coupled with control circuit interfaces. He also serves as a reviewer for conferences and journals curated by the IEEE Circuits and Systems Society. His research is funded by CONNECT, the Science Foundation Ireland Research Center for Future Networks and Communications. His research interests include modeling and simulation methods of multi-physics and nonlinear systems, high-performance computation, and time series analysis.



DIMITRI GALAYKO (Member, IEEE) graduated from Odessa State Polytechnic University, Ukraine, in 1998. He received the master's degree from the Institut of Applied Sciences of Lyon (INSA-Lyon, France), in 1999, and the Ph.D. degree from University Lille-I, in 2002. He made his Ph.D. thesis with the Institute of Microelectronics and Nanotechnologies (IEMN), Lille, France. The topic of his Ph.D. dissertation was the design of microelectromechanical silicon filters and resonators for radio-communications. Since 2005, he has been an Associate Professor with the LIP6 Lab, Sorbonne University. He is the coauthor of two books on kinetic energy harvesting. His research interests include study, modeling, and design of nonlinear integrated circuits for sensor interface and for mixed-signal applications. His expertise includes modeling and design of systems for kinetic energy harvesters and design of circuits for synchronisation and clocking. He has served for several conferences and journals of IEEE CASS Society (an Associate Editor for IEEE TRANSACTIONS ON CIRCUITS AND SYSTEMS—II: EXPRESS BRIEFS (TCAS-II) and IEEE OPEN JOURNAL OF CIRCUITS AND SYSTEMS (OJCAS), a Technical Program Chair for IEEE ICECS Conference, and a track chair for several CASS conferences).



MICHAEL PETER KENNEDY (Fellow, IEEE) received the B.E. degree in electronics from the National University of Ireland, Dublin, Ireland, in 1984, the M.S. and Ph.D. degrees from the University of California (UC Berkeley), Berkeley, in 1987 and 1991, respectively, and the D.Eng. degree from the National University of Ireland, in 2010.

He worked as a Design Engineer with Philips Electronics, a Postdoctoral Research Engineer with the Electronics Research Laboratory, UC Berkeley, and a Professeur Invité with the Federal Institute of Technology Lausanne (EPFL), Switzerland. From 1992 to 2000, he was on the faculty of the Department of Electronic and Electrical Engineering, University College Dublin (UCD), Dublin, where he taught electronic circuits and computer-aided circuit analysis and directed the undergraduate Electronics Laboratory. In 2000, he joined University College Cork (UCC), Cork, Ireland, as a Professor and the Head of the Department of Microelectronic Engineering. He was the Dean of the Faculty of Engineering, UCC, from 2003 to 2005, and the Vice-President for Research from 2005 to 2010. He returned to UCD as a Professor of microelectronic engineering in 2017, where he is currently the Head of the School of Electrical and Electronic Engineering. He was made an IEEE Fellow in 1998 for his contributions to the study of Neural Networks and Nonlinear Dynamics. He has served on the IEEE Fellow Committee and the IEEE Gustav Robert Kirchhoff Award Committee. He was a recipient of the 1991 Best Paper Award from the *International Journal of Circuit Theory and Applications* and the 1999 Best Paper Award from the European Conference on Circuit Theory and Design. He was awarded the IEEE Third Millennium Medal, the IEEE Circuits and Systems Society Golden Jubilee Medal in 2000, and the inaugural Parson's Medal for Engineering Sciences by the Royal Irish Academy (RIA) in 2001. He was elected to membership of the RIA in 2004, served as the RIA Policy and International Relations Secretary from 2012 to 2016, and as the President in 2017. He was the Vice-President for Region 8 of the IEEE Circuits and Systems Society (CASS) from 2005 to 2007, a CASS Distinguished Lecturer from 2012 to 2013, and the Chair of the CASS Distinguished Lecturer Program in 2017. He has also served as an Associate Editor for the IEEE TRANSACTIONS ON CIRCUITS AND SYSTEMS from 1993 to 1995 and from 1999 to 2004.



ELENA BLOKHINA (Senior Member, IEEE) received the Habilitation (HDR) degree in electronic engineering from UPMC Sorbonne Universities, France, in 2017, and the M.Sc. degree in physics and the Ph.D. degree in physical and mathematical sciences from Saratov State University, Russia, in 2002 and 2006, respectively.

From 2005 to 2007, she was a Research Scientist with Saratov State University. Since 2007, she has been with the School of Electrical and Electronic Engineering, University College Dublin, Ireland, where she is currently an Associate Professor and the Coordinator of the Circuits and Systems Research Group. Her research interests include the analysis, design, modeling, and simulations of nonlinear circuits, systems and networks with particular application to complex, mixed-domain, and multi-physics systems. She had been elected to serve as a member of the boards of governors of the IEEE Circuits and Systems Society for the term 2013–2015 and has been re-elected for the term 2015–2017. She has served as a member for organising committees, review and programme committees, a session chair, and a track chair for many leading international conferences on circuits, systems and electronics, including the IEEE International Symposium on Circuits and Systems. She is also the Chair of the IEEE Technical Committee on Nonlinear Circuits and Systems. She has also served as the Programme Co-Chair for the first edition of IEEE Next Generation of Circuits and Systems Conference 2017, the Programme Co-Chair for the IEEE International Conference on Electronics, Circuits and Systems (ICECS) 2018, and the General Co-Chair for IEEE ICECS 2020. From 2016 to 2017, she was an Associate Editor of the IEEE TRANSACTIONS ON CIRCUITS AND SYSTEMS—I: REGULAR PAPERS. Since 2018, she has been the Deputy Editor in Chief of that Journal.

• • •